A Numerical Investigation of Power Extraction using Biomimetic Hydrofoils for a Full Passive Oscillating Hydrokinetic Turbine

Ramon III Gregorio
Aerospace Engineering Department, Ateneo de Davao University

Cylvia Mae Gonzaga
Aerospace Engineering Department, Ateneo de Davao University

Jonathan Maglasang
Ateneo de Davao University

https://doi.org/10.5109/7323348

出版情報：Proceedings of International Exchange and Innovation Conference on Engineering & Sciences (IEICES). 10, pp.773-778, 2024-10-17. International Exchange and Innovation Conference on Engineering & Sciences
バージョン：

A Numerical Investigation of Power Extraction using Biomimetic Hydrofoils for a Full Passive Oscillating Hydrokinetic Turbine

Ramon III Gregorio[1], Cylvia Mae Gonzaga[1], Jonathan Maglasang[2]
[1]Aerospace Engineering Department. Ateneo de Davao University
[1]Ateneo de Davao University/Cebu Technical University
Corresponding email: rp3gregorio@gmail.com

Abstract: *A new concept of hydrokinetic turbines based on oscillating hydrofoils using the biomimetic foils Dragonfly Canard and NREL-S814 comparing its power performance to that of a standard NACA 0015 foil is conducted in this study through the use of 2D simulations using URANS with Spalart-Allmaras as a turbulence model. The fluid conditions used in the study include U_∞=2 m/s, ρ=997 kg/m^3, Re = 500,000, a chord length of 0.25 m, Φ=90°, and θo=75° across all foils. The dimensionless frequency is f*=0.14, f*=0.20, and f*=0.12 were used across 3 cases. The heaving amplitudes used for Case 1&2 is Ho = c, while Case 3 is Ho=2c. The study gives insight into the advantages and disadvantages of using biomimetic foils. A symmetrical foil is observed to provide the best-performing foils in CP and η results. Additionally, increasing the foil's frequency and heaving amplitude decreases flow detachment, improving the overall performance.*

Keywords: CFD, Oscillating Hydrokinetic Turbine, Biomimetic Hydrofoils, URANS, Ocean Renewable Energies

1. INTRODUCTION

The world's expanding energy consumption and population growth have slowed the exploration of natural resources, with many countries relying on non-renewable energy sources to boost their economies [1]. This has been a problem for decades since the primary non-renewable energy sources known are the most prominent contributing pollutants worldwide [2]. Burning these fossil fuels contribute to carbon emissions that have long-term and short-term effects on the environment [3]. There has been a lot of attempts to harness renewable energies to name a few the use of VAWT in Highway Traffic Vehicles [4] and even a Solar, Wind and Biomass-Based Hybrid Renewable Energy System [5]. Another potential would be harnessing power from stream current energy could be a significant energy source to those areas near the coastline, providing them with a dependable and more stable energy source. Flow velocities on tropical sites have typical values of less than 2 m/s [6]. On the other hand, the country has low flow velocities, which means introducing a Hydrokinetic Turbine is viable in some coastal areas [7]. Ocean wave energy is a concentrated type of solar energy due to winds created by the pressure difference in the Earth's atmosphere [8]. Harnessing the potential of Ocean Energy can contribute to the stabilization of electricity supply in Asia and the Pacific

An Oscillating Hydrokinetic Turbine is a turbine based on Oscillating Hydrofoils that extract energy from water currents that are induced by either tides or gravity. This technology is well suited for riverbeds and shallow waters near the coasts due to its rectangular extraction plane, allowing the possibility to scale up the rated power by simply increasing the turbine hydrofoil span [9]. Moreover, the untwisted hydrofoils in the oscillating turbines have simpler geometry and are easier to produce than usual rotor blades. An Oscillating hydrokinetic turbine extracts power from the kinematic motion of flapping hydrofoils with two degrees of freedom, converting it to a rotating motion to power a generator while restricted to a pitching axis located on the chord line at the position of "xp" from the leading edge [10]. The following figure below represent the oscillating motion of the hydrofoil [9].

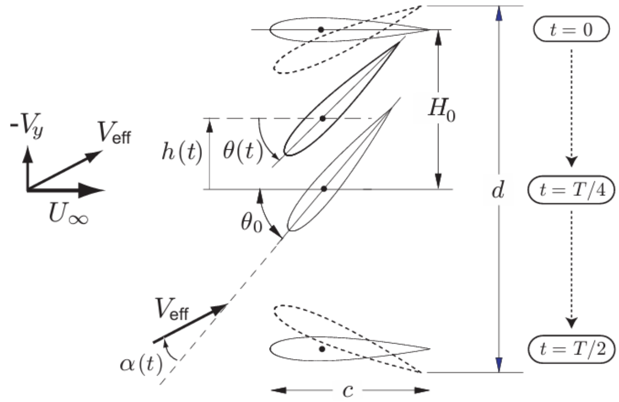

Fig 1. Oscillating Foil Movement

Where the pitching and heaving amplitudes are represented by θ_o and H_o, respectively; the pitching and heaving velocities are represented Ω by and V_o; the angular frequency is represented by (γ=2πf), and the phase difference between the two motions is represented by Φ. A symmetrical NACA 0015 foil was used in the figure, wherein "c" represents the chord length and d is the total y-axis displacement distance, maintaining a phase angle to be 90 degrees. The oscillating airfoil's freestream velocity further upstream is U_∞.

The study's general objective is to conduct an analytical and numerical approach to determine the hydrodynamic properties of the different biomimetic and control hydrofoils geometries. The findings of these approaches will aid future studies to create a laboratory model to verify the results gathered from the study. The parameters that will be collected are the Lift, Drag, Moment, Power Coefficients and Percent Efficiency. The gathered data will give insight into how varying parameters (frequency, heaving amplitude, and foil geometry) affect in the overall performance of the foil.

This study will mainly identify and contrast the possible electrical power output of the Biomimetic foils compared to that of the control foil using numerical simulation and analytical results.

The study will have the following specific objectives:

1. Evaluate the baseline hydrodynamic performance of the control foil (NACA 0015) using theoretical approach and verifying its 2D geometry distribution through CFD analysis as well as perform a flow visualization using ANSYS Fluent.
2. Compare the hydrodynamic performance of the biomimetic-inspired hydrofoils (Dragon Fly Canard and NREL S814) to that of the control foil (NACA 0015) through CFD analysis.
3. Compare and investigate the results in Coefficient of Power and percent efficiency of the biomimetic-inspired hydrofoils (Dragon Fly Canard and NREL S814) to that of the control foil (NACA 0015).

2. METHODOLOGY

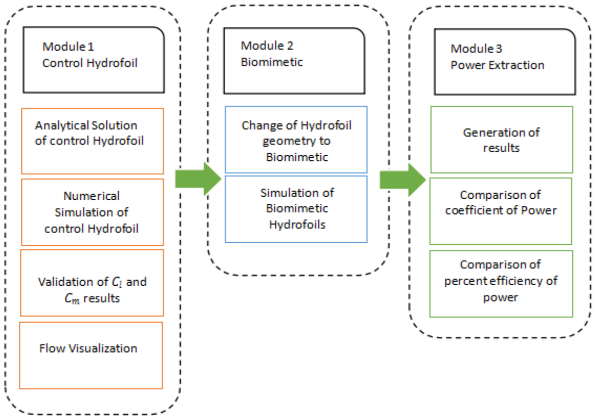

Fig 2. Research Design Diagram

The first module of the study will focus on the numerical simulations of the control hydrofoil and the creation of the analytical solution to validate the results of the numerical simulations setup using Ansys Fluent with the Quasi-Steady and the Theodorsen Theory. The second module will then focus on simulations of the Biomimetic Hydrofoils and the effects of the different cases on the hydrodynamic properties of hydrofoils. The simulations will then gather data about C_L, C_M, C_p, and percent efficiency results. The collected data will then be compared to the data obtained from the control hydrofoil (NACA 0015). Lastly, module 3 will then focus on comparing the Cp and percent efficiency produced by the three (3) hydrofoils tested and determine which produces the most efficient electrical power output.

2.1 Input Parameters

The following cases will be used in comparing the hydrodynamic and power generation performance of the control foil. The analytical results are based on the steady-state assumption and unsteady-state theory.

Table 1. Case parameter set-ups

Case	1	2	3
Hydrofoil		NACA 0015/Dragonfly/ NREL S814	
Length (c)		0.25 m	
Pitching Axis (xp)		c/3	
Heaving Amplitude	c	c	2c
Pitching Amplitude		75°	
Motion Phase		90°	
Flow Speed		2 m/s	
Fluid Density		997 (kg/m^3)	
f	1.12	1.6	0.96
Dimensionless frequency	0.14	0.20	0.12
Strouhal Significance	0.14	0.20	0.24
Time for one Cycle	0.893 s	0.625 s	1.042 s
α_{max}	33.66°	23.51°	18.55°

2.2 Meshing Set-Up

Dynamic Mesh was used in the study. The flow field of the hydrofoil was determined in comparison to its chord length. A setup from Kinsey and Dumas [24] stated that the upper and lower flow fields should be 35 times the size of the chord from the origin. The left side of the flow field where the incoming flow is from should be 35 times the size of the chord length, and the right side for the outflow should be 40 times the size of the chord length from the origin. The unsteady formulation is based on a first-order implicit scheme, which is imposed from the use of dynamic mesh capabilities.

The hydrofoils motion is prescribed via User-Defined Functions (UDFs) compiled and linked to the solver. Dynamic meshes and sliding non-conformal interfaces allow relative motion of adjacent mesh zones. Each hydrofoil is encapsulated in a circular mesh region which has a diameter of 2.36C, moving in a rigid body with them and allowing to preserve the grid quality in the critical near-body and boundary-layers mesh zones. These circular mesh sectors are each enclosed in a large mesh zone heaving in phase with the foils. To allow relative motions between all these cell zones, non-conformal sliding interfaces are used. One is required for each foil at the limit of its near-body circular mesh zone. Another one is needed at the linear interface between both heaving cell regions. Finally, the cells adjacent to the computational domain external boundaries are deforming, playing the role of a buffer mesh area to allow the heaving cell zone motion.

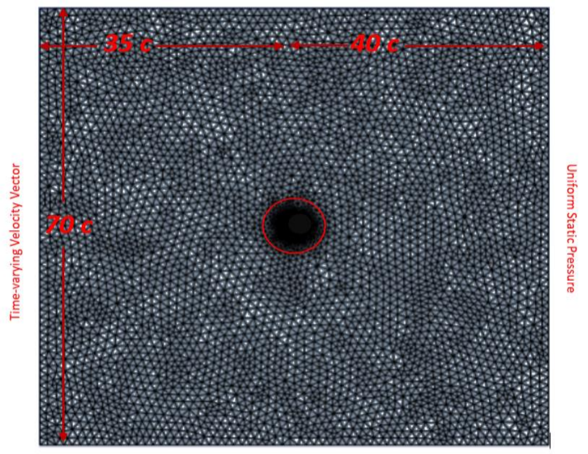

Fig 3. 2D Boundary Conditions for Test set-up

A flow field with a width of 70 times the chord length and a length of 75 times of the chord length was sketched in the Design Modeler. The domain was divided into two zones bounded by a circular non-conformal sliding interface in preparation for a dynamic mesh. This approach attaches the heaving reference frame or the vertical translation to the hydrofoil. The pitching portion of the hydrofoil motion is left so the hydrofoil is rotating in the translating reference frame. This implies using time-varying velocity conditions on the inflow domain boundary and adding a new source term in the Navier-Stokes equation to account for the reference-frame acceleration.

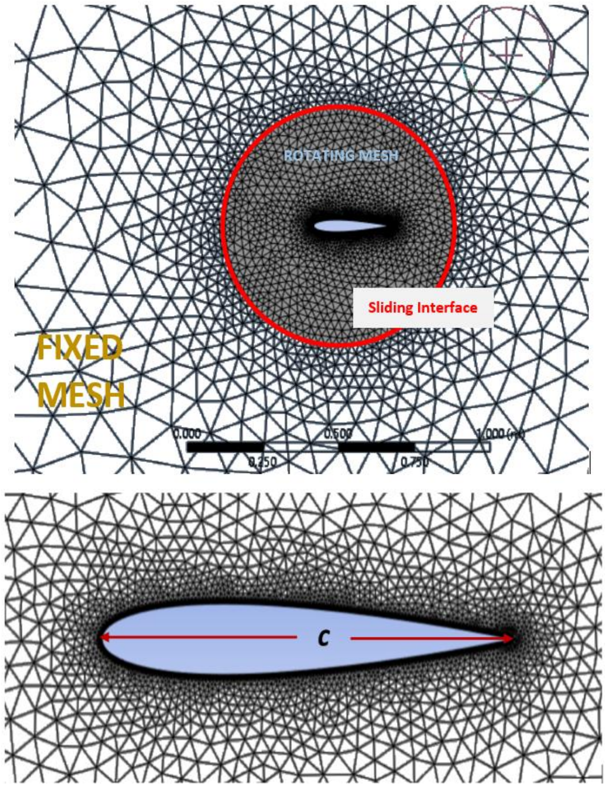

Fig 4. a. Non-conformal Sliding Interface, b. Mesh over the Hydrofoil

The Dynamic mesh and the sliding non-conformal interface allow relative motion of adjacent mesh zones. The hydrofoil motion is prescribed via User-Defined Functions (UDFs) compiled and linked to the solver. A non-conformal sliding interface centered on the hydrofoil pitching center is used to allow relative motion between the hydrofoil near-body mesh zone and the external mesh zone. This accounts for the pitching part of the oscillating motion.

3. RESULTS AND DISCUSSION

The data generated for this study was done using ANSYS Fluent with three (3) varying geometries and three (3) input parameters for each hydrofoil coded in the User Defined Function and compiled in ANSYS Fluent's Compiler. This step allowed for a continuous simulation run changing only the Reduced frequency and the Heaving Amplitude Values in the UDF code. The extracted performance data was presented in a graph form in preparation for the analysis and comparison of calculations. The values obtained from the hydrodynamic performance of the control hydrofoil would be tabulated and used to plot the graphs for the coefficients of lift, momentum, and power and the percent efficiency versus dimensionless time. After the data processing and visualization, the results for the Coefficient of Lift were compared with the numerical results from the study that used the control hydrofoil. The flow conditions of this experiment were also applied in this numerical simulation, including Re and flow velocity. In addition, Figure 3.8 shows the CL values from the study of Kinsey and Dumas [9] and the Numerical Setup.

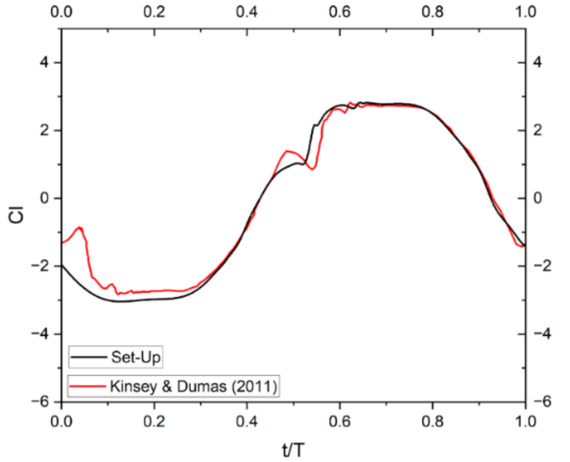

Fig 5. Coefficient of Lift from the numerical study of Kinsey and Dumas and the set-up results

Throughout the cases, the results follow the trend from the Analytical solution. The results are also closer to that of the analytical solution provided by the Theodorsen theory, which agrees with the notion that it is a more accurate solution than that of the quasi-steady function. The peak results cases are the following: Case 1 (CL = 2.828, CM = 0.594), Case 2 (CL = 3.915, CM = 0.903), and Case 3 (CL = 2.407, CM = 0.580). The mean results per case are the following: Case 1 (CL = -0.343, CM = -0.054), Case 2 (CL = 0.0193, C¬M = 1.82E-05), and Case 3 (CL = 0.0052, CM = -0.0017). It is also to be noted that the graphs become smoother in Case 2 and Case 3 conditions as compared to that of Case 1.

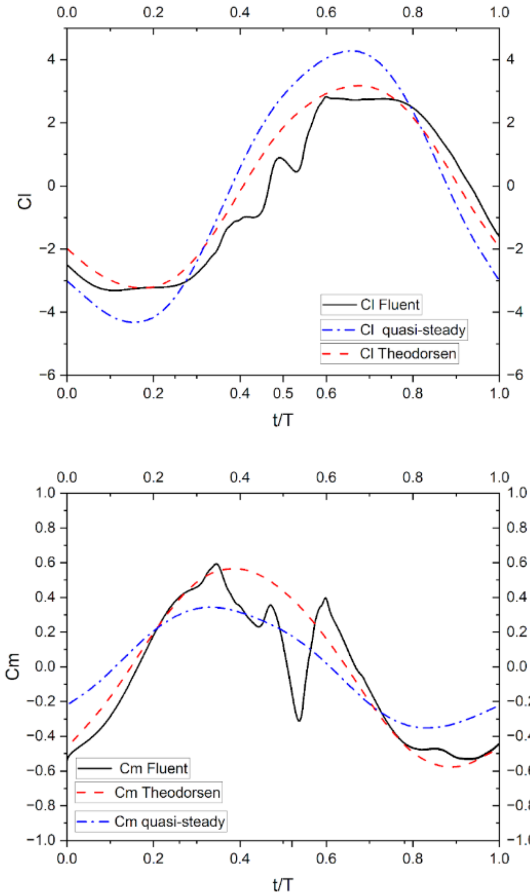

Fig 6. Analytical Solutions vs Set-up (Case 1)

This is because, with an increase in the dimensionless frequency and plunging amplitudes, the foils lead to development in fluid-structure interactions. The fluctuations found in Case 1 can be attributed to the difficulty in maintaining a non-stall condition by the foil during stroke reversals.

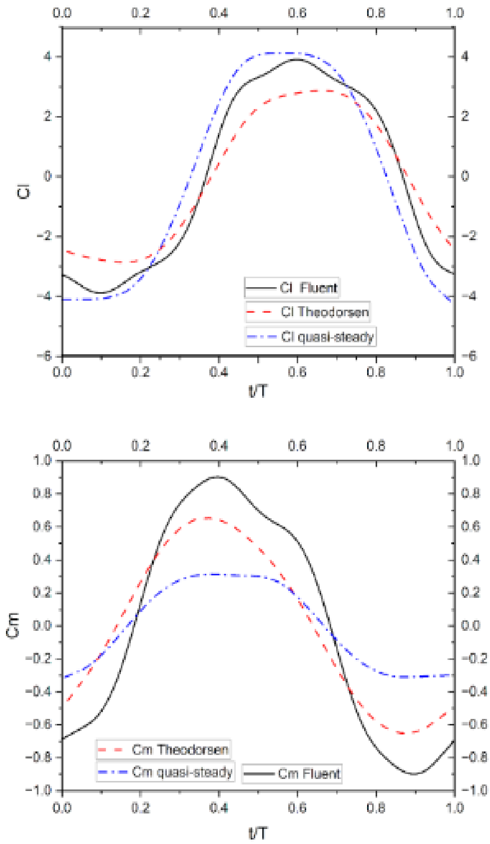

Fig 7. Analytical Solutions vs Set-up (Case 2)

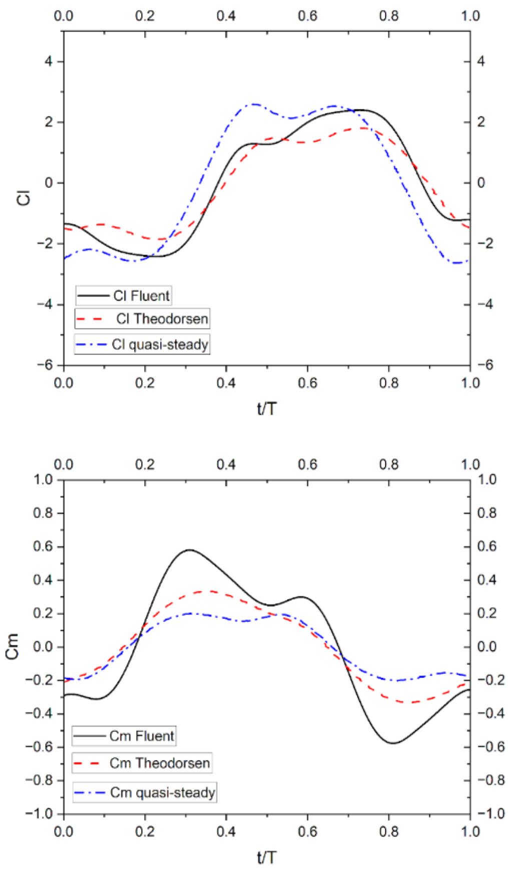

Fig 8. Analytical Solutions vs Set-up (Case 3)

3.1 Biomimetic Hydrofoil Performance

For case 1, the best-performing foil is the symmetrical hydrofoil (NACA 0015) in both efficiency and CP generation. Since its upper and lower surfaces are the same in both upstroke and downstroke, the foil's performance is relatively the same. The biomimetic foils find it difficult to generate power when approaching stroke reversal. This is because it experiences dynamic stalling and incomplete vortex shedding. The Dragonfly Canard, because of its flat lower surface, has the lowest generated power during the downstroke. At upstroke, the foil has a higher mean performance given that it is positively cambered. The second-best performing foil is the NREL S814, as it is upper and lower camber are more near symmetrical than the Dragonfly Canard, its performance is slightly lower than that of the NACA 0015.

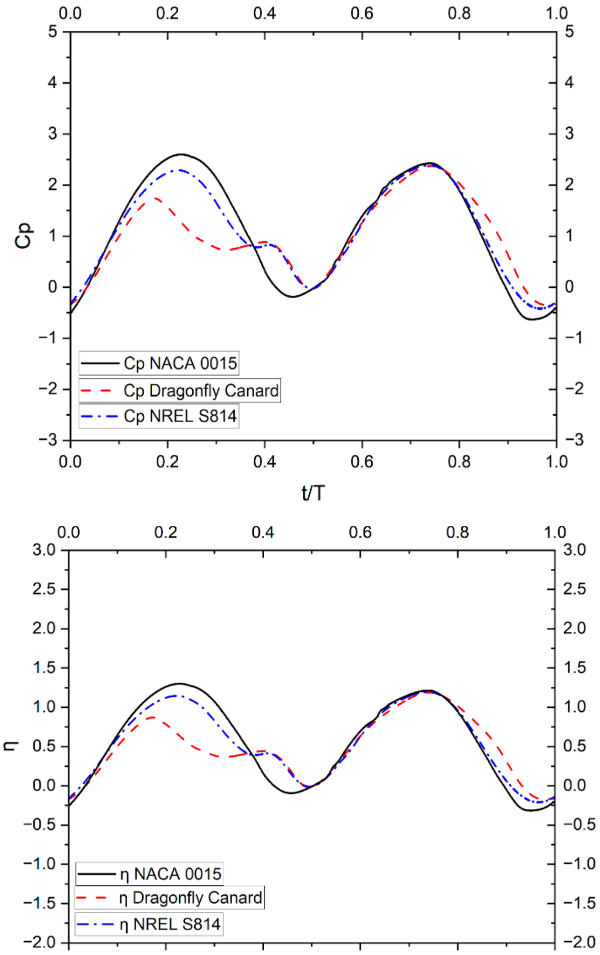

Fig 9. Comparison of Case 1 Hydrofoil Performance ($f* = 0.14$, $\theta_o = 75°$, $H_o = c$) a. Coefficient of Power, b. Percent Efficiency

For this case 2, the best-performing foil is the symmetrical (NACA 0015) in efficiency and CP generation. Since its upper and lower surfaces are the same. It is also evident that the foil's upstroke and downstroke performance are relatively the same. The increase in frequency has led to significant improvements in the performance of the foils compared to Case 1. This is because the foil is given more time to develop fluid-structure interactions. For the Dragonfly Canard, it can be seen that the increase in frequency made its cp and percent generation start earlier, and due to it having a positively cambered foil, the upstroke performance of the foil is the highest compared to the other foils. The NREL

S814 is the second-best performing foil with closer results than the NACA 0015. It can be noted as well that both the biomimetic foils have lower negative performance at the aft of the cycle, because of their upper surface profile.

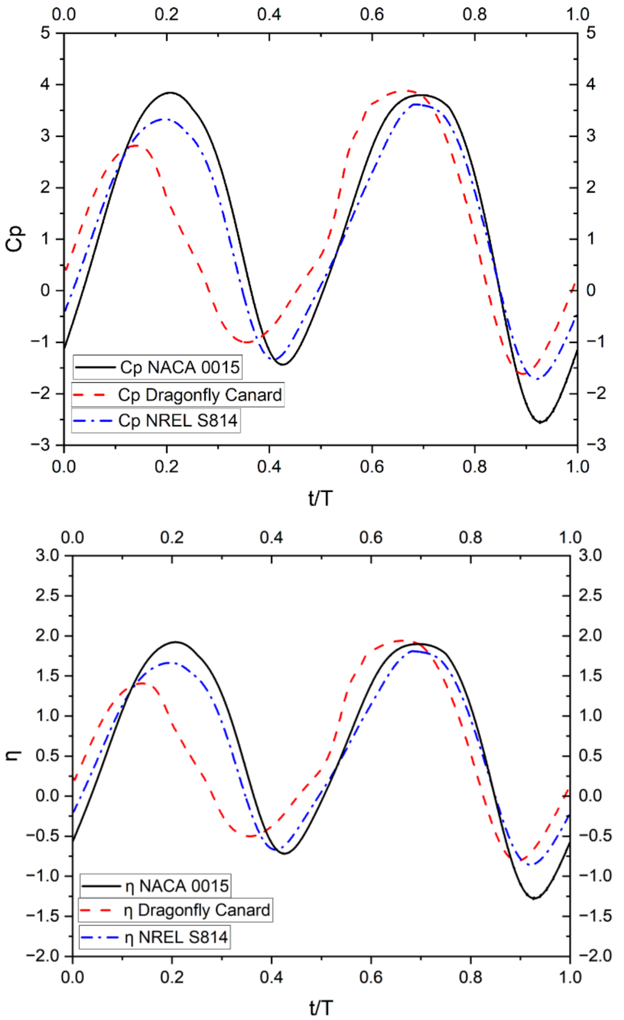

Fig 10. Comparison of Case 1 Hydrofoil Performance ($f_* = 0.12$, $\theta_0 = 75°$, $H_0 = c$) a. Coefficient of Power, b. Percent Efficiency

In case 3, it can be seen that the best-performing foil is symmetrical (NACA 0015) in both efficiency and CP generation. It is also evident that the foil's upstroke and downstroke performance is relatively the same. The increase in heaving amplitude has greatly benefited the upstroke performance of the Dragonfly Canard, having a higher maximum value than the other foils. However, its downstroke performance is the lowest compared to the other foils. The NREL S814 is seen to have the best performance during stroke reversal and is the second-best performing foil. Due to the increase in amplitude, the percent efficiency for case 3 is the lowest among all cases across all foils because the available stream power also increases. It can be noted as well that both the biomimetic foils have lower negative performance at the aft of the cycle, because of their upper surface profile.

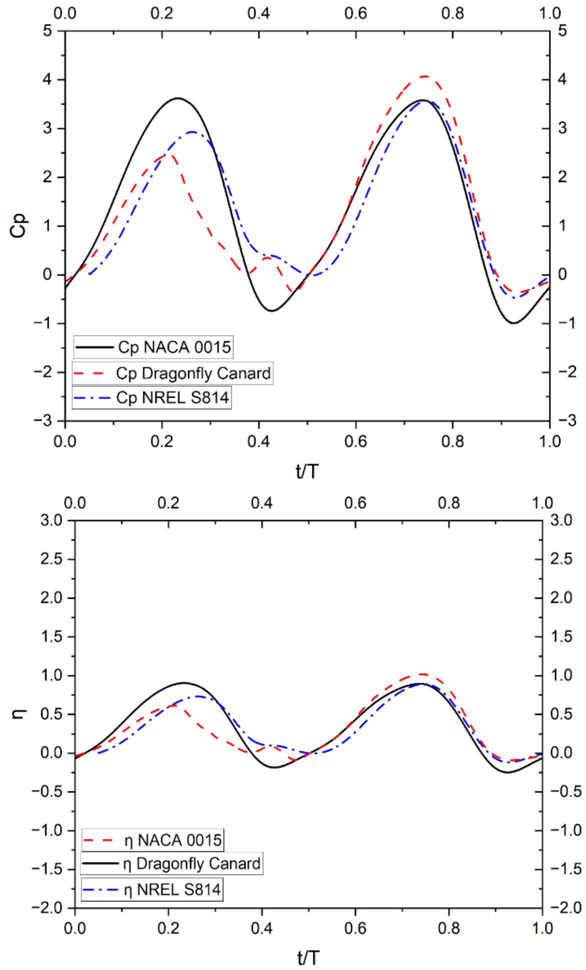

Fig 11. Comparison of Case 3 Hydrofoil Performance ($f_* = 0.12$, $\theta_0 = 75°$, $H_0 = 2c$) a. Coefficient of Power, b. Percent Efficiency

4. CONCLUSION

Although case 3 has the best maximum CP performance among all foils, case 2 has the best percent efficiency performance with similar results. Case 1 has the least amount of CP generated but still provides a higher percent efficiency than case 3. This because the foil experience detachment from having lower frequencies in its cycles. It can also be seen that for the NACA 0015, a symmetrical foil, the value of the average cm is close to zero across the 3 cases. This is because of its profile being symmetrical; the downstroke and upstroke CM forces cancel each other. It can be observed as well that during the time 0.5 in all foils and cases, the power generation diminishes to nearly 0; this is because, at this point, the foil experiences a momentary loss of motion, thus not producing power.

In summary, to acquire results for the CP and percent efficiency, a code was used to assess the hydrodynamic performance of the foil as motion is induced in the foil. The software used for the simulations is ANSYS FLUENT, via 2D URANS simulation using Spalart-Allmaras as the turbulence model. There were three configurations used, which gave insight into the power-generating performance comparison between the biomimetic hydrofoils and the control hydrofoil. Case 3 for all hydrofoils foils has resulted in the highest peak

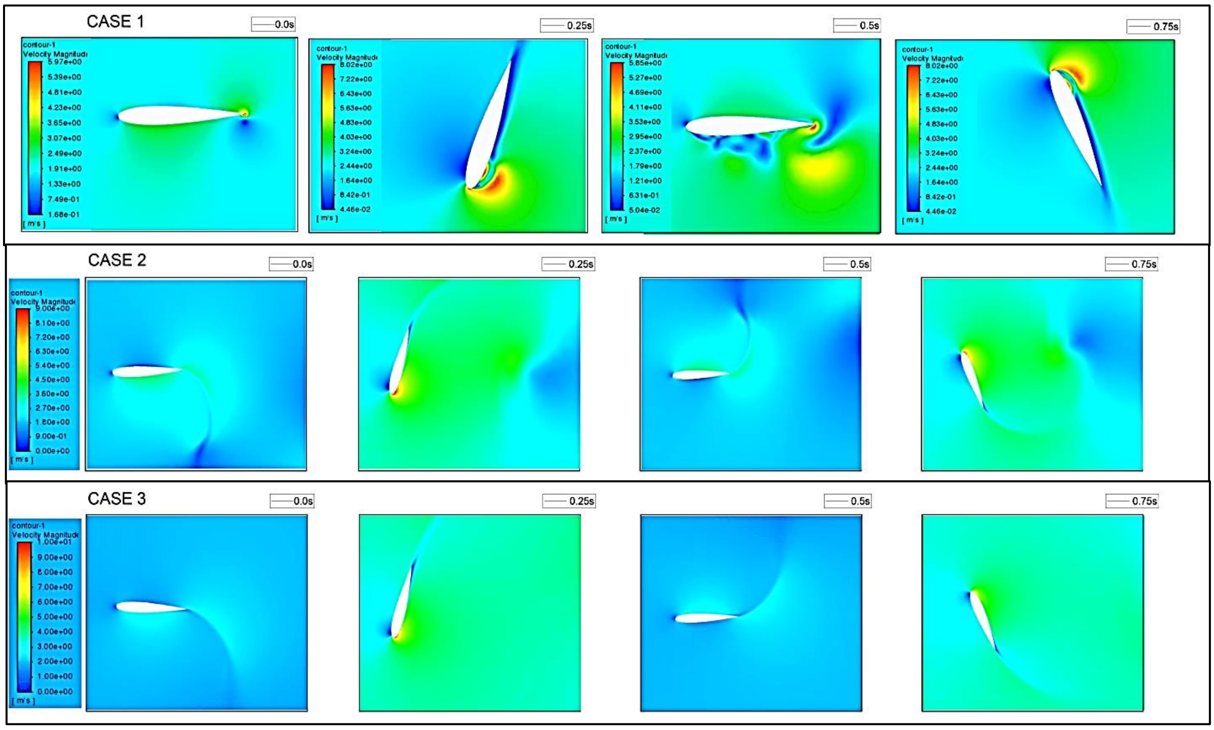

Fig 12. Flow Visualization of NACA 0015 across the 3 cases (link to video: https://youtu.be/k_caPPtUa6E)

performances in average CP. However, Case 2 is observed to be the best performing with the highest percent efficiency while not being far from the cp performance of Case 3.

4.1 Recommendations

The proponents of this study suggest that future researchers try different parameters and find the most suitable set-ups to the biomimetic foils. It was observed that an increase in pitching and plunging amplitudes, a change in phase angle, and reduced frequency. Thick foils should still be considered so that its durability would not be in question for an experimental study. A change in Reynolds number would also be best to study the effects of the foils in both laminar and turbulent flows. An application of flexibility to the foils would also be best to further improve performance by utilizing the wake vortices forces. Optimization of the setup for the biomimetic hydrofoils should also be considered to grasp the full potential of the geometry of the hydrofoils used in this study. It would also be best for future studies to use symmetrical biomimetic foils and introduce corrugation for 2D tandem and 3D simulations. An addition of scalability for of results using dimensional analysis and similitude would be ideal as well in both 2D and 3D simulations.

5. REFERENCES

[1] Saiqa Naz et al., Rashida Sultan, "Moderating and mediating role of renewable energy consumption, FDI inflows, and economic growth on carbon dioxide emissions: evidence from robust least square estimator," Environmental Science and Pollution Research (2018)

[2] F. Perera, Pollution from Fossil-Fuel Combustion is the Leading Environmental Threat to Global Pediatric Health and Equity: Solutions Exist, Int J Environ Res Public Health, (2017) vol. 15, no. 1, p. 16

[3] E. Andriesse, "Persistent fishing amidst depletion, environmental and socio-economic vulnerability in Iloilo Province, the Philippines," Ocean Coast Manag, vol. 157, (2018) pp. 130–137

[4] Shoel Rana, Biplob Roy, Bidyut Baran Saha, Sampad Ghosh. Energy Harvesting from Highway Traffic Vehicles Movement via VAWT In Proceedings of International Exchange and Innovation Conference on Engineering & Sciences (IEICES). 8, (2022) pp.122-127

[5] A.D. Avi, T. Fayaz, B.B. Saha, S. Ghosh, Optimization of Solar, Wind and Biomass-Based Hybrid Renewable Energy System in St. Martin's Island, Bangladesh, In Proceedings of International Exchange and Innovation Conference on Engineering & Sciences (IEICES). 7 (2021) 122–128.

[6] J. I. Encarnacion, C. Johnstone, and S. Ordonez-Sanchez, "Design of a Horizontal Axis Tidal Turbine for Less Energetic Current Velocity Profiles," J Mar Sci Eng, doi: 10.3390/jmse7070197. (2019), vol. 7, no. 7, p. 197

[7] M. Rotor and H. Hefazi, "Design and Simulation of a Horizontal-Axis Tidal Turbine (HATT) Blades for Tropical Site Conditions using Reynolds-Averaged Navier-Stokes - Blade Element Momentum Theory (RANS-BEMT)," (2021)

[8] M. R. D. Quitoras, M. L. S. Abundo, and L. A. M. Danao, "A techno-economic assessment of wave energy resources in the Philippines," Renewable and Sustainable Energy Reviews, vol. 88, doi: 10.1016/j.rser.2018.02.016. (2018), pp. 68–81

[9] T. Kinsey and G. Dumas, "Analysis, Optimization And Demonstration Of A New Concept Of Hydrokinetic Turbine Based On Oscillating Hydrofoils," (2011)

[10] J. M. Anderson, K. Streitlien, D.S. Barret, and M.S. Triantafyllou, "Oscillating foils of high propulsive efficiency," (1998)